and of the subsequent cycles varies to a lesser extent. The heat stored within the system and the heat released from it per cycle converge rapidly toward the stabilized cycle values.

6) The addition of interdigitated heat-conducting fins to the heat-storage system reduces the q_0 excursions at the end of the melting. The energy stored in the material of the fins cannot be neglected, but the additional degrees of freedom provided by the choices of fin material, make it possible to synchronize the thermal cycling of the system with orbital cycles.

References

[1] Martinek, F., "Investigation of Heat Transfer Process in Solar Energy Storage Systems for Space Applications," Ph.D. thesis, 1966, Univ. of Cincinnati.

[2] Stefan, J., "Ueber die Theorie der Eisbildung in Polarmeere," *Annalen der Physik and Chemie*, Vol. 42, 1891, p. 269

[3] Altman, M., "Prospects for Thermal Energy Storage," *AGARD'ograph 81*, Gordon & Breech, New York, 1967, pp. 135–149.

[4] Altman, M., "The Determination of Thermal Energy Diffusivities of Thermal Energy Storage Materials," *Transactions of the ASME, Ser. A: Journal of Engineering for Power*, Vol. 89, 3, July 1967, pp. 407–414.

[5] Cygnarowicz, T. A. and Gibson, R. N., "Design and Performance of a Thermal Storage Resistoret," *Journal of Spacecraft and Rockets*, Vol. 5, No. 6, June 1968, p. 686.

[6] Sutton, G. W., "The Hydrodynamics and Heat Conduction of a Melting Surface," *Journal of the Aerospace Sciences*, Vol. 25, No. 1, Jan. 1958, pp. 29–32.

[7] Tripp. C. N., "Volatile Liquid Pressurization," *Journal of Spacecraft and Rockets*, Vol. 5, No. 12, Dec. 1968, p. 1477.

[8] Douglas, J., and Gallie, T. M., "On the Numerical Integration of a Parabolic Differential Equation Subject to a Moving Boundary Condition," *Duke Math. Journal*, Vol. 22, 1955, Duke Univ., Durham, N. C., p. 577.

[9] Murray, W. D., "Numerical and Machine Solutions of Problems in Transient Heat Conduction," Ph.D. thesis, 1958, New York Univ., College of Engineering.

[10] Price, P. H. and Slack, M. R., "Stability and Accuracy of Numerical Solutions of Heat Flow," *British Journal, Applied Physics*, Vol. 3, 1952, p. 379.

[11] Citron, S. J., "Heat Conduction in a Melting Slab," Ph.D. thesis, 1959, Columbia Univ.

[12] Cochran, D. L., "Rate of Solidification, Application and Extension of Theory." T-R 24, Contract N6NONr-251, 1955, Stanford Univ., Stanford, Calif.

[13] Evans, G. W., Isaacson, E., and MacDonald, J. K. L., "Stefan-like Problems," *Quarterly of Applied Mathematics*, Vol. 8, 1950, pp. 312–319.

[14] Hrycak, P., "Problem of Solidification with Newton's Cooling at the Surface," *AIChE Journal*, Vol. 9, No. 5, 1963, pp. 585–589.

[15] Ruoff, A. L., "An Alternare Solution of Stefan's Problem," *Quarterly of Applied Mathematics*, Vol. 16, July, 1958, pp. 197–201.

SEPTEMBER 1970 J. SPACECRAFT VOL. 7, NO. 9

Aerodynamic First-Order Method for Flexible Bodies

George F. McCanless Jr.*
Chrysler Corporation, Huntsville, Ala.

This paper develops an advanced method of computing aerodynamic forces that act on flexible launch vehicles and missiles in supersonic flight. The procedure is an extension of the rigid-body, first-order method. The equation of the perturbation velocity potential is first expressed in rigid Cartesian coordinates. It is then transformed into flexible-body coordinates to simplify the boundary conditions. The transformed aerodynamic boundary value problem for flexible bodies is solved to yield the stream velocities at body surfaces. The velocities then determine the surface pressures and hence the body forces. Sample calculations for a flexed cone and for a flexed Saturn V vehicle demonstrate that significant aerodynamic forces are induced by forebody flexing.

Nomenclature

a_i	= constants of the supersonic source strength derivatives, fps
b_i	= constants of the supersonic doublet strength derivatives, fps
C_N	= normal force coefficient
C_p	= pressure coefficient
D	= base diameter, ft
f	= supersonic source strength, ft^2/sec
m	= supersonic doublet strength, ft^2/sec
M	= Mach number
M_{cg}	= pitching moment about the center of gravity, ft lb
N	= normal force, lb
N'	= local normal force, lb/ft
p	= arbitrary point in space
q	= dynamic pressure, lb/ft^2
r	= radial coordinate in flexible-body coordinate system, ft
R	= body radius, ft
s	= dummy integration variable
U,u	= velocities in the X and x directions, fps
V,v	= velocities in the Y and r directions, fps
W,w	= velocities in the Z and θ directions, fps
x	= flexible-body axial coordinate, ft
X,Y,Z	= Cartesian coordinates, ft
$\bar{Z}$	= displacement of flexible-body axis in the cartesian coordinate system, ft
α	= local angle of attack, rad
α_r	= rigid-coordinate angle of attack, rad
β	= Mach number parameter
γ	= specific heat ratio
θ	= flexible-body circumferential coordinate, rad
$\Lambda_{n,i}$	= parameter defined by Eq. (25)
ν	= number of body stations
$\Xi_{n,i}$	= parameter defined by Eq. (26)
ϕ	= perturbation velocity potential, ft^2/sec

Received June 16, 1969; revision received March 31, 1970. This study was supported by the Aero-Astrodynamics Laboratory of NASA Marshall Spaceflight Center under contract NAS8-21290. J. G. Papadopoulos was the program Contracting Officer's Representative.

* Engineering Specialist. Member AIAA.

$\psi_{n,i}$ = parameter defined by Eq. (24)
$\Omega_{n,i}$ = parameter defined by Eq. (38)

Superscript

$'$ = derivative with respect to x, 1/ft

Subscripts

a,c = axial flow and cross flow
cg,cp = centers of gravity and pressure, respectively
i,j,n = body station indices
∞ = freestream

Introduction

THE aerodynamic forces generated by the flexing of large launch vehicles and missiles can cause catastrophic failures unless these forces are properly accounted for in the design of these vehicles and missiles. This paper develops an advanced method of computing the aerodynamic characteristics of flexible bodies in the supersonic regime. The need for increased precision in determining the forces was established in studies of vehicle flight dynamics by Papadopolous.[1,2] Vehicle flexibility causes complex behavior of structures and control systems. A portion of the increased complexity arises because the aerodynamic forces that act at a body station depend not only on the local angle of attack but also on the angles of attack of upstream stations. Consequently, the deflected shapes of the entire bodies must be considered in determining aerodynamic loadings. A theoretical method for describing the aerodynamic effects of flexing is needed, because it may be impractical to construct a representative number of flexed wind-tunnel models. The flexible-body aerodynamic forces must be determined early in development programs, so that they can be included in the design of structures and control systems. Utilizing these design factors will prevent direct structural failures and loss of control.

Previous calculations of the aerodynamic characteristics of flexible bodies have been made with the slender-body method as extended by Dahm.[3] Unfortunately, its accuracy is limited and it does not account for variations in Mach number. Another technique consists of modifying rigid-body aerodynamic force distributions. In this technique the local-normal-force derivatives of rigid bodies with respect to angle of attack (α) are established by solving the boundary value problems of rigid bodies. The solutions are frequently determined by the rigid-body, first-order method or the second-order, shock-expansion method. The method of characteristics is also used to obtain exact solutions of the nonlinear partial differential equation of inviscid flow. Alternatively, the local-normal-force derivatives of rigid bodies can be determined experimentally. In both cases the local normal forces that act on flexible bodies are determined by multiplying rigid-body local-normal-force derivatives by the local α's of the flexible bodies. Use of this technique implicitly requires the unrealistic assumption that the local normal forces acting at a station on a flexible body are the same as those which would exist at this station if the forward portion of the vehicle were rigid. Furthermore, it requires that the hypothetical rigid forward portion be at the same α as the station being analyzed.

In the following sections an advanced method of computing the aerodynamic forces that act on flexible bodies is developed that includes the effect of Mach number variations. The computation procedure is an extension of the aerodynamic first-order method described by Ferri[4] and Van Dyke.[5] It consists of determining solutions of the flexible-body boundary value problems instead of modifying solutions of the rigid-body boundary value problems. Solving flexible-body boundary value problems consists of obtaining solutions of the partial differential equation of the perturbation velocity potential ϕ and then evaluating these solutions so that they satisfy the flexible-body boundary conditions. This requires that the surface velocities of the computed flow must be exactly tangent to the body surfaces. However, the descriptions of the tangency conditions at the surfaces of flexible bodies in rigid cylindrical and cartesian coordinates are complex. To simplify the descriptions of these boundary conditions, the equation of ϕ is transformed from cartesian coordinate systems to the inherent flexible-body coordinate systems. The boundary conditions are also expressed in the new systems. The flexible-body coordinate systems are similar to cylindrical systems; the principle difference is that the flexible centerlines of the launch vehicles or missiles replace the rigid cylindrical axes. The method is then developed to satisfy the partial differential equation and the simplified boundary conditions expressed in flexible-body coordinates. The solutions of these transformed boundary value problems yield the ϕ's from which the velocity components are obtained. The velocity components are inserted in the exact pressure relation to yield the pressures on body surfaces.

The computation procedure derived in this paper is applicable to pointed bodies when the body cross flow is uniform and the variations in α are due only to body flexing. The derivation is for supersonic attached flow about bodies of revolution, but the method can be used for bodies with fins by increasing body diameter to generate forces equivalent to those contributed by fins. The method, although developed for computing steady-state aerodynamic forces, can be used for determining the characteristics of slowly oscillating bodies when the aerodynamic terms are virtually independent of time. Each oscillating launch vehicle or missile must be studied as a separate case to establish the amplitudes and frequencies over which this method is applicable.

Flexible Body Coordinates

Aerodynamic calculations of the flow about bodies consist of determining solutions of boundary value problems. In this section the inherent coordinate systems of flexible bodies are developed from cartesian coordinates as shown in Fig. 1. The partial differential equation of ϕ is transformed into the new coordinate system, and the boundary conditions are expressed in them to simplify the boundary value problem.

Let us consider first the flexible-body boundary value problem expressed in the rigid X, Y, Z cartesian coordinate system of Fig. 1. The perturbation velocity potential $\phi(X, Y, Z)$ must satisfy the supersonic partial differential equation

$$-\beta^2(\partial^2\phi/\partial X^2) + \partial^2\phi/\partial Y^2 + \partial^2\phi/\partial Z^2 = 0 \qquad (1)$$

and it must also satisfy the boundary conditions imposed by the flexible body. Here the body nose is located at the origin of the coordinate system and the flexible-body centerline, which lies in the $Y = 0$ plane, is distributed along the X axis. The freestream velocity U_∞ also lies in the $Y = 0$ plane. Define the rigid coordinate angle of attack α_r as the angle formed by the freestream velocity vector and the X axis. Then the U, V, and W velocity components in the X, Y, and Z directions are given by

$$U = U_\infty \cos\alpha_r + \partial\phi/\partial X \qquad (2)$$

$$V = \partial\phi/\partial Y \qquad (3)$$

$$W = U_\infty \sin\alpha_r + \partial\phi/\partial Z \qquad (4)$$

The inherent coordinate system of a flexible body shown in Fig. 1 is next determined in terms of this cartesian system. In addition, the equation of the perturbation velocity potential is transformed into the new coordinate system and the boundary conditions are expressed in it. Consider a point p and pass a plane through this point perpendicular to the flexible-body centerline. The distance along the centerline to this plane is the flexible-body axial (x) coordinate. The distance in the constructed plane from this axial coordinate to the point p is the flexible-body radial (r) coordinate. A line is defined by the intersection of the constructed plane and the $Y = 0$ plane.

The angle between this line and the radial coordinate is the flexible-body circumferential (θ) coordinate. The flexible-body coordinates (x, r, θ) are given in terms of the rigidy-body coordinates (X, Y, Z) by the following equations, which are restricted to cases where the deflections $\bar{Z}$ of the flexible-body centerline and their derivatives, $d\bar{Z}/dX$, are small

$$x = X + (d\bar{Z}/dX)Z \tag{5}$$

$$r = [Y^2 + (Z - \bar{Z})^2]^{1/2} \tag{6}$$

$$\theta = \tan^{-1}[Y/(Z - \bar{Z})] \tag{7}$$

Equation (1) is transformed into flexible-body coordinates using the chain rule of partial differentiation and partial derivatives from Eqs. (5–7):

$$-\beta^2 \frac{\partial^2\phi}{\partial x^2} + \frac{\partial^2\phi}{\partial r^2} + \frac{1}{r}\frac{\partial\phi}{\partial r} + \frac{1}{r^2}\frac{\partial^2\phi}{\partial\theta^2} = \beta^2 \frac{\partial(d^2\bar{Z}/dX^2)}{\partial x} r\cos\theta \frac{\partial\phi}{\partial x} \tag{8}$$

To extend the aerodynamic first-order method it is necessary that the form of the transformed equation of ϕ be identical to the form of the equation when expressed in rigid cylindrical coordinates. This requires that the right-hand side of Eq. (8) must be negligible compared to the left-hand side. The term on the right is negligible for launch vehicles and missiles because the derivatives of the body curvature with respect to distance, $\partial(\partial^2\bar{Z}/\partial X^2)/\partial x$, are small. From elementary beam theory the derivatives of curvature of a flexing structure are proportional to the shearing forces. Computations of the derivatives of the curvature from the shearing forces show that they are generally small. The requirement of negligible values of the right-hand side of Eq. (8) yields the transformed supersonic partial differential equation ϕ;

$$-\beta^2 \frac{\partial^2\phi}{\partial x^2} + \frac{\partial^2\phi}{\partial r^2} + \frac{1}{r}\frac{\partial\phi}{\partial r} + \frac{1}{r^2}\frac{\partial^2\phi}{\partial\theta^2} = 0 \tag{9}$$

The velocity components in the flexible-body coordinate system are given by equations similar to those in the rigid-body systems with the local angles of attack α replacing the rigid coordinate angles of attack α_r. The u, v, and w velocity components in the x, r, and θ directions of the flexible-body coordinate system are:

$$u = U_\infty \cos\alpha + \partial\phi_a/\partial x + \partial\phi_c/\partial x \tag{10}$$

$$v = U_\infty \sin\alpha \cos\theta + \partial\phi_a/\partial r + \partial\phi_c/\partial r \tag{11}$$

$$w = -U_\infty \sin\alpha \sin\theta + (1/r)\partial\phi_c/\partial\theta \tag{12}$$

where ϕ_a and ϕ_c are the axial-flow and cross-flow perturbation potentials. The sum of these two potentials yields the total perturbation velocity potential ϕ.

The potentials are also required to satisfy the boundary conditions at the surface of the flexible body. Here the flow at the body surfaces must be exactly tangent to the surfaces. This requirement is expressed:

$$(dr/dx)_R = (v/u)_R \tag{13}$$

where R is the body radius at station x. Substituting Eqs. (10) and (11) yields:

$$\left(\frac{dr}{dx}\right)_R = \left(\frac{U_\infty \sin\alpha \cos\theta + \partial\phi_a/\partial r + \partial\phi_c/\partial r}{U_\infty \cos\alpha + \partial\phi_a/\partial x + \partial\phi_c/\partial x}\right)_R \tag{14}$$

This equation is exactly satisfied, if the two potentials satisfy the following equations:

$$\left(\frac{dr}{dx} U_\infty \cos\alpha\right)_R = \left(\frac{\partial\phi_a}{\partial r}\right)_R - \left(\frac{dr}{dx}\frac{\partial\phi_a}{\partial x}\right)_R \tag{15}$$

$$(U_\infty \sin\alpha)_R = \left(\frac{dr}{dx}\frac{1}{\cos\theta}\frac{\partial\phi_c}{\partial x}\right)_R - \left(\frac{1}{\cos\theta}\frac{\partial\phi_c}{\partial r}\right)_R \tag{16}$$

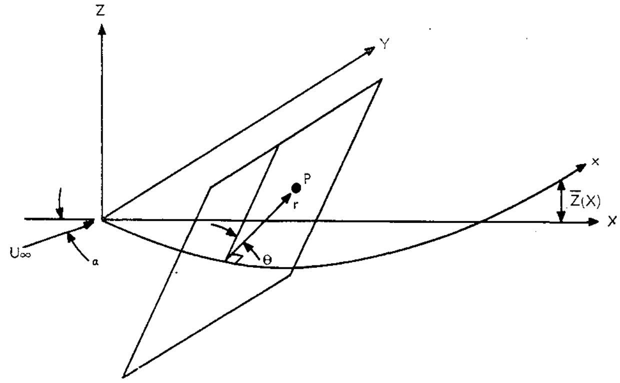

Fig. 1 Flexible-body coordinate system.

The significance of the two equations in the flexible-body coordinate system is that the first contains only ϕ_a, which is independent of θ, and the second contains only ϕ_c, which is, however, dependent on θ.

First-Order Solution for Flexible Bodies

General axial and cross-flow perturbation velocity potentials are given here. They are solutions of the supersonic partial differential equation expressed in flexible-body coordinates of ϕ, Eq. (9). The potentials are then evaluated so that they also satisfy the flexible-body boundary conditions given by Eqs. (15) and (16).

The following ϕ_a has been shown to satisfy the equation of ϕ. It is obtained by integrating the supersonic source distribution along the body axis from the nose to the Mach cone that emanates from the axis and intersects the point (x,r).

$$\phi_a(x,r) = \int_{\cosh^{-1}(x/\beta r)}^{0} f(x - \beta r \cosh s)ds \tag{17}$$

where $f(0) = 0$ for pointed bodies, because the body nose cannot propagate disturbances upstream in supersonic flow. To complete the solution of the boundary value problem, the derivatives of the supersonic sources distribution f' must be evaluated so that the boundary conditions at discrete points along the surface of the body are satisfied. In determining the derivatives at these points, the body surface is divided into a sequence of body stations (x_i,r_i) as shown in Fig. 2, with $i = 1$ designating the body nose. The following perturbation velocities in the axial and radial directions at station n are obtained by taking the derivatives of ϕ_a:

$$\left(\frac{\partial\phi_a}{\partial x}\right)_n = \int_{\cosh^{-1}(x_n/\beta r_n)}^{0} f'(x_n - \beta r_n \cosh s) \times ds - \frac{f(0)}{\beta r_n[(x_n/\beta r_n)^2 - 1]^{1/2}} \tag{18}$$

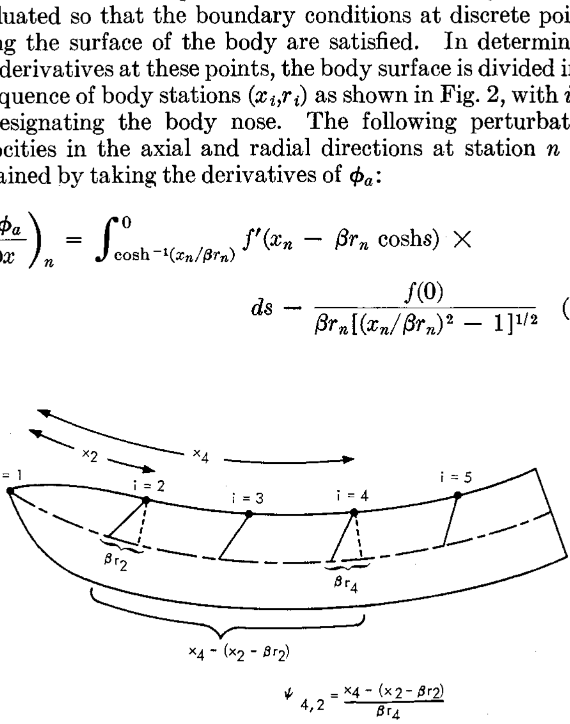

Fig. 2 Geometry of flexible bodies.

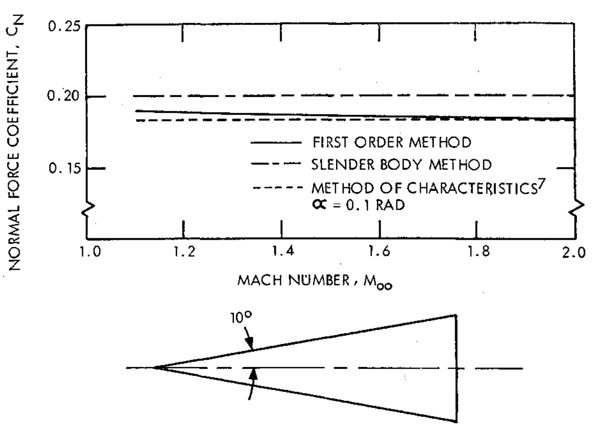

Fig. 3 Normal force on rigid cone.

$$\left(\frac{\partial\phi_a}{\partial r}\right)_n = -\beta\int_{\cosh^{-1}(x_n/\beta r_n)}^{0} f'(x_n - \beta r_n \cosh s) \times \cosh s\, ds + \frac{f(0)(x_n/\beta r_n)}{r_n[(x_n/\beta r_n)^2 - 1]^{1/2}} \quad (19)$$

The last term in each of these equations is zero since $f(0) = 0$. Now let the source derivatives f' be constants over intervals along the axis of the body according to the following relation:

$$f'(x_n - \beta r_n \cosh s) = a_i \quad (20)$$

for values of s, such that

$$(x_{i-1} - \beta r_{i-1}) < (x_n - \beta r_n \cosh s) \le (x_i - \beta r_i) \quad (21)$$

To evaluate the constants a_n substitute the previous expressions into Eqs. (18) and (19):

$$\left(\frac{\partial\phi_a}{\partial x}\right)_n = \sum_{i=2}^{n} a_i\Lambda_{n,i} \quad (22)$$

$$\left(\frac{\partial\phi_a}{\partial r}\right)_n = -\beta\sum_{i=2}^{n} a_i\,\Xi_{n,i} \quad (23)$$

where the following definitions have been used:

$$\psi_{n,i} = [x_n - (x_i - \beta r_i)]/\beta r_n \quad (24)$$

$$\Lambda_{n,i} = \cosh^{-1}\psi_{n,i} - \cosh^{-1}\psi_{n,i-1} \quad (25)$$

$$\Xi_{n,i} = (\psi^2_{n,i} - 1)^{1/2} - (\psi^2_{n,i-1} - 1)^{1/2} \quad (26)$$

The term $\psi_{n,i}$ is illustrated in Fig. 2. Inserting Eqs. (22) and (23) into the exact tangency conditions given by Eq. (15) yields the following equation for evaluating the constants of the supersonic source strength derivatives a_n at discrete points:

$$a_n = \frac{-\left(\dfrac{dr}{dx}U_\infty\cos\alpha\right)_n - \sum_{i=2}^{n-1} a_i\left[\beta\Xi_{n,i} + \left(\dfrac{dr}{dx}\right)_n\Lambda_{n,i}\right]}{\beta\Xi_{n,n} + (dr/dx)_n\Lambda_{n,n}} \quad (27)$$

Here $a_1 = 0$, because of the properties of pointed bodies in supersonic flow. The constants a_n are used in Eqs. (22) and (23) to determine the perturbation velocity components generated by ϕ_a.

A similar procedure is used to determine the velocity components generated by ϕ_c. It has also been shown[6] to satisfy the equation of ϕ. It is obtained by integrating the supersonic doublet distribution along the body axis from the nose to the Mach cone that emanates from the axis and intersects the point (x,r):

$$\phi_c(x,r,\theta) = -\cos\theta\cdot\beta \times \int_{\cosh^{-1}(x/\beta r)}^{0} m(x - \beta r\cosh s)\cosh s\, ds \quad (28)$$

where $m(0) = 0$ for pointed bodies in supersonic flow. The supersonic doublet distribution m and its derivatives m' must be evaluated so that the tangency conditions, given by Eq. (16), are satisfied at discrete points on the body surface. To evaluate these terms, determine the perturbation velocity components at station n that are generated by ϕ_c by taking the derivatives of ϕ_c:

$$\left(\frac{\partial\phi_c}{\partial x}\right)_n = -\cos\theta\cdot\beta\int_{\cosh^{-1}(x_n/\beta r_n)}^{0} m'(x_n - \beta r_n\cosh s) \times \cosh s ds + \frac{m(0)\cos\theta\cdot(x_n/\beta r_n)}{r_n[(x_n/\beta r_n)^2 - 1]^{1/2}} \quad (29)$$

$$\left(\frac{\partial\phi_c}{\partial r}\right)_n = \cos\theta\cdot\beta^2\int_{\cosh^{-1}(x_n/\beta r_n)}^{0} m'(x_n - \beta r_n\cosh s) \times \cosh^2 s ds - \frac{m(0)\cos\theta\cdot\beta(x_n/\beta r_n)^2}{r_n[(x_n/\beta r_n)^2 - 1]^{1/2}} \quad (30)$$

$$\frac{1}{r_n}\left(\frac{\partial\phi_c}{\partial\theta}\right)_n = \frac{\sin\theta}{r_n}\beta\int_{\cosh^{-1}(x_n/\beta r_n)}^{0} m(x_n - \beta r_n\cosh s) \times \cosh s ds \quad (31)$$

The last term in each of the first two equations is zero since $m(0) = 0$. Let the supersonic doublet distribution be represented by

$$m(x_n - \beta r_n\cosh s) = \beta r_n\left[-b_i\cosh s + \sum_{j=2}^{i}(b_j - b_{j-1})\psi_{n,j-1}\right] \quad (32)$$

where the terms b_i are constants over restricted intervals. The derivative is given by

$$m'(x_n - \beta r_n\cosh s) = b_i \quad (33)$$

Both equations are valid for values of s, such that

$$(x_{i-1} - \beta r_{i-1}) < (x_n - \beta r_n\cosh s) \le (x_i - \beta r_i) \quad (34)$$

These equations are next substituted into Eqs. (29–31) to initiate the evaluation of the supersonic doublet constants b_n

$$\left(\frac{\partial\phi_c}{\partial x}\right)_n = -\cos\theta\cdot\beta\sum_{i=2}^{n} b_i\Xi_{n,i} \quad (35)$$

$$\left(\frac{\partial\phi_c}{\partial r}\right)_n = \frac{1}{2}\cos\theta\cdot\beta^2\sum_{i=2}^{n} b_i(\Lambda_{n,i} + \Omega_{n,i}) \quad (36)$$

$$\frac{1}{r_n}\left(\frac{\partial\phi_c}{\partial\theta}\right)_n = \frac{1}{2}\sin\theta\cdot\beta^2\sum_{i=2}^{n}\left[2\left\{\sum_{j=2}^{i}(b_j - b_{j-1})\psi_{n,j-1}\right\} \times \Xi_{n,i} - b_i\{\Lambda_{n,i} + \Omega_{n,i}\}\right] \quad (37)$$

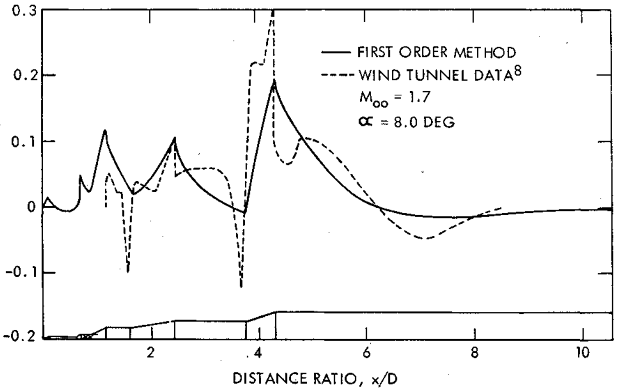

Fig. 4 Local normal force distribution on rigid Saturn V.

where $\Omega_{n,i}$ is defined as

$$\Omega_{n,i} = \psi^2{}_{n,i}(\psi^2{}_{n,i} - 1)^{1/2} - \psi_{n,i-1}(\psi^2{}_{n,i-1} - 1)^{1/2} \quad (38)$$

and $\psi_{n,i}\Lambda_{n,i}$, and $\Xi_{n,i}$ are defined by Eqs. (24–26). The determination of the supersonic doublet constants b_n are completed by substituting Eqs. (35) and (36) into the tangency conditions given by Eq (16)

$$b_n = \frac{-2(U_\infty \sin\alpha)_n - \beta \sum_{i=2}^{n-1} b_i[2(dr/dx)_n\Xi_{n,i} + \beta(\Lambda_{n,i} + \Omega_{n,i})]}{\beta[2(dr/dx)_n\Xi_{n,n} + \beta(\Lambda_{n,n} + \Omega_{n,n})]} \quad (39)$$

Because of the properties of pointed bodies in supersonic flow' the strength of the derivatives of the doublet at the body nose is zero and this results in $b_1 = 0$. The cross-flow perturbation components are determined by inserting these values of the constants b_n into Eqs. (35–37).

The total velocity components are determined by Eqs. (10–12) using both the axial and cross-flow potentials. The total velocity components are then used to evaluate the pressure coefficient at the body stations. The exact expression for the pressure coefficient is:

$$C_{pn}(\theta) = \frac{2}{\gamma M_\infty^2}\left[\left\{1 + \frac{\gamma - 1}{2} M_\infty^2 \times \left(1 - \frac{u_n^2 + v_n^2 + w_n^2}{U_\infty^2}\right)\right\}^{\gamma/(\gamma-1)} - 1\right] \quad (40)$$

The local normal forces, the normal force, the pitching moment about the center of gravity, and the center of pressure measured from the nose are given by

$$N_n' = -2qr_n \int_0^\pi C_{pn}(\theta) \cos\theta d\theta \quad (41)$$

$$N = \sum_{n=2}^{\nu-1} N_n' \left(\frac{x_{n+1} - x_{n-1}}{2}\right) \quad (42)$$

$$M_{cg} = \sum_{n=2}^{\nu-1} N_n'(x_{cg} - x_n)\left(\frac{x_{n+1} - x_{n-1}}{2}\right) \quad (43)$$

$$x_{cp} = x_{cg} - M_{cg}/N \quad (44)$$

These equations are the solution of the flexible-body boundary value problem expressed in flexible-body coordinates and they constitute the first-order method for flexible bodies. It is similar to the rigid-body first-order method with the local angles of attack replacing the rigid-body angles of attack. It is applicable to rigid bodies, since rigid bodies are special cases of flexible bodies. The first-order method for flexible bodies reduces to the extended slender body method when the slender body restrictions are imposed. The method of this paper includes variations in Mach number and also includes the effects of forebody deflection.

Results

The results of calculations made with the first-order method for flexible bodies are described in this section. The objective of these calculations is to provide a basis for comparison of the method with those previously in use and to determine the nature of the aerodynamic forces generated by body flexing. Results are given for a rigid cone and a rigid Saturn V vehicle. Also included are results for a flexed cone and a flexible Saturn V vehicle which illustrate the phenomenon of aerodynamic forces induced by forebody flexing.

The local normal forces acting on a rigid cone have been calculated. The method of this paper is applicable, since a rigid body is a special case of a flexible body. Twenty-five body stations were used in obtaining the results shown in Fig. 3. This large number of body stations is required by the

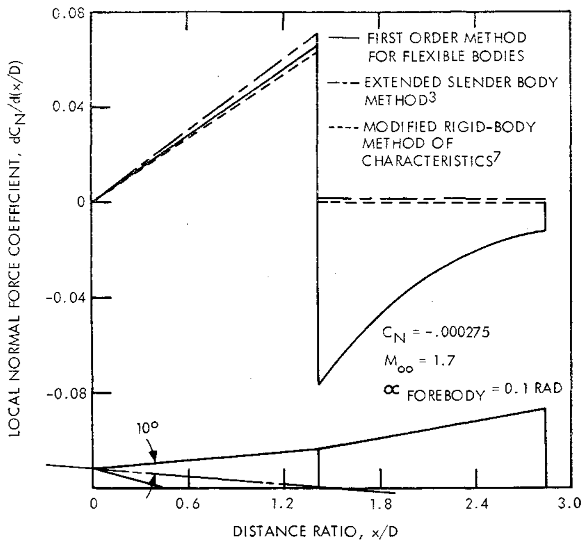

Fig. 5 Local normal force distribution on flexible cone.

numerical integration technique used to compute the normal force. Also shown are the results based on the slender-body method and the method of characteristics. The results[7] from the latter method are exact solutions of the nonlinear equation of the velocity potential. The values computed by the method of this paper are less than the values estimated by the slender body method. However, they are in excellent agreement with exact results.

Calculations have been made for a rigid Saturn V vehicle without fins by the method of this paper. Sixty-nine body stations were used. Figure 4 gives these results as well as the results of wind tunnel tests.[8] Agreement is good; the areas of over-calculation compensated those of under-calculation. The computed results appear to be "smoothed" versions of the experimental results. The differences are caused by the asymmetry in the regions of separated flow. Wind-tunnel optical systems show that these regions are generated by the frustum sections at moderate angles of attack. The calculations illustrate that this method gives valid results for rigid launch vehicles.

A flexed cone shown in Fig. 5 has been analyzed. This cone is selected because of its simplicity even though the intersection of its fore and aft portion is abrupt. Because of this severe change in body slope, this problem does not strictly comply with the requirement of negligible values of the right-hand side of Eq. (8). The requirement could be met by replacing this cone with a similar one which has a more gradual change in slope and the aerodynamic forces acting on the two would be virtually identical. Calculations have been made by this method using 25 body stations. These results and those determined by the extended slender body method are given in Fig. 5. It also shows the results obtained by the

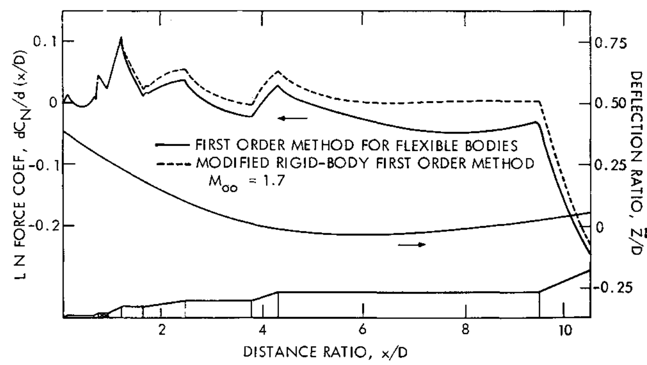

Fig. 6 Local normal force distribution on flexible Saturn V.

technique of using the method of characteristics to establish the aerodynamic force distribution acting on a rigid cone and then modifying the distribution for the flexible-body case.

Calculations for the fixed cone by the three methods yield similar forebody force distributions. The slender-body method gives larger forces than the other two methods. The significant differences are displayed at the afterbody. The method of this paper indicates that the forebody induces large negative local normal forces on the afterbody. This phenomenon of aerodynamic forces induced by forebody flexing is caused by the afterbody "straightening" the flow that has been "turned" by the flexing of the forebody. The slender-body method yields a negative "spike" at the intersection followed by zero local normal forces on the afterbody. The technique of modifying the rigid-body force distribution yields no disturbance at the intersection and simply results in zero local normal forces on the afterbody. Although the slender-body method does give a spike, neither it nor the technique of modifying the rigid-body force distribution demonstrate the phenomenon of aerodynamic forces induced by forebody flexing. The results of applying this method must be tempered because of the abrupt intersection of the fore and aft portions of the cone. However, this method is shown to provide increased precision in computing flexible body forces and to illustrate an aerodynamic phenomenon that is not indicated by the previous methods.

Finally, the method of this paper has been used to compute the aerodynamic forces acting on a flexed Saturn V vehicle with fins. The results given in Fig. 6 are based on 69 body stations. Flexible body results are also shown that were determined by the technique of modifying the rigid-body force distribution obtained by the rigid-body, first-order method. In both cases an axially symmetric frustum is added to the Saturn V vehicle to simulate the fin-shroud combination. The local normal forces on the aft portion of the vehicle when computed by the method of this paper are substantial. However, these forces are virtually zero when determined by modifying the rigid-body force distribution. As in the previous example, this illustrates the phenomenon of aerodynamic forces induced by the forebody flexing which is caused by the turning and straightening of the airstream. Applying the first-order method for flexible bodies to a flexed launch vehicle yields greater accuracy and also illustrates an aerodynamic phenomenon that has been generally disregarded.

Conclusions and Recommendations

The preceding analysis and calculations have shown that the transformation of aerodynamic boundary value problems into flexible-body coordinate systems simplifies the boundary conditions. This simplification facilitates the extension of the first-order method to solve the flexible-body boundary value problems. However, its application is restricted to cases in which changes in curvature are small. The method of this paper yields results which have greater accuracy than those obtained by the extended slender-body method and by the technique of modifying rigid-body characteristics. The phenomenon of aerodynamic forces induced by forebody flexing is caused by the turning of the airflow by the forebody and its straightening by the afterbody.

It is recommended that the first-order method for flexible bodies be extended to include the effects of separated flow, and that the method of this paper be extended to include time-dependent phenomena.

References

[1] Papadopoulos, J. G., "Aeroelastic Load Growth Effects on Saturn Configurations," TM-X-53634, July 1967, NASA.

[2] Papadopoulos, J. G., "Wind Penetration Effects on Flight Simulations," AIAA Paper 67–609, Huntsville, Ala., 1967.

[3] Dahm, W. K., "Approximate Longitudinal Normal Force Distribution on Slender Bodies and Body-Tail Configurations, Oscillating in Arbitrary Mode Shapes," Aeroballistics Internal Note 80, Nov. 1955, Guided Missile Development Division, Redstone Arsenal, Huntsville, Ala.

[4] Ferri, A., *Elements of Aerodynamics of Supersonic Flows*, 1st ed., Macmillan, New York, 1949, Chap. 11.

[5] Van Dyke, M. D., "First-and Second-Order Theory of Supersonic Flow Past Bodies of Revolution," *Journal of the Aeronautical Sciences*, Vol. 18, No. 3, March 1951, pp. 161–178.

[6] McCanless, G. F. and Bradley, D., "Study Program of Local Angle-of-Attack Effects on Vehicle Dynamic Response," HSM-R111-68, Oct. 1968, Chrysler Huntsville Operations, Huntsville, Ala.

[7] Ames Research Staff, "Equations, Tables, and Charts for Compressible Flow," Rept. 1135, 1953, NACA.

[8] "Static Aercdynamic Characteristics of the Apollo-Saturn V Vehicle," TMX-53517, Sept. 1966, NASA.